Nanostructured Ultrathin Films of Alternating Sexithiophenes and Electropolymerizable Polycarbazole Precursor Layers Investigated by Electrochemical Surface Plasmon Resonance (EC-S...

ARTICLE *in* LANGMUIR · AUGUST 2008

Impact Factor: 4.46 · DOI: 10.1021/la800307u · Source: PubMed

Thin Solid Films 518 (2010) 2200–2205

Contents lists available at ScienceDirect

Thin Solid Films

journal homepage: www.elsevier.com/locate/tsf

Nanostructured carbon nanotubes/copper phthalocyanine hybrid multilayers prepared using layer-by-layer self-assembly approach

Akira Baba [a,*], Yoshinori Kanetsuna [a], Saengrawee Sriwichai [a,b], Yasuo Ohdaira [a], Kazunari Shinbo [a], Keizo Kato [a], Sukon Phanichphant [b], Futao Kaneko [a]

[a] Center for Transdisciplinary Research, and Graduate School of Science and Technology, Niigata University, 8050 Ikarashi 2-nocho, Nishi-ku, Niigata 950-2181, Japan
[b] Department of Chemistry, Faculty of Science, Chiang Mai University, Chiang Mai 50200, Thailand

ARTICLE INFO

Article history:
Received 16 January 2009
Received in revised form 1 September 2009
Accepted 11 September 2009
Available online 19 September 2009

Keywords:
Layer-by-layer
Surface plasmon
Carbon nanotubes
Composites
Cyclic voltammetry
Multilayered ultrathin film

ABSTRACT

In this report, we demonstrate a convenient method of fabricating single-walled carbon nanotubes/organic semiconductor hybrid ultrathin multilayers using a layer-by-layer self-assembly approach. Single-walled carbon nanotubes were solubilized by water-soluble cationic alcian blue pyridine variant and anionic copper phthalocyanine-3,4′,4″,4‴-tetrasulfonic acid tetrasodium salt, which were then utilized for electrostatic layer-by-layer multilayer fabrication. The solubilization ability of single-walled carbon nanotubes was studied in water by UV–vis absorption spectroscopy. The composites were highly dispersed owing to the π–π interactions. *In situ* surface plasmon resonance spectroscopy during the layer-by-layer multilayer fabrication indicated a stepwise increase in reflectivity, indicating the successive formation of nanostructured hybrid ultrathin films. Cyclic voltammetry revealed that the electroactivity of the hybrid film was enhanced by the incorporation of single-walled nanotubes.

1. Introduction

There has been a great deal of interest in the fabrication of nanostructured assemblies of carbon nanotube-organic composites for a wide range of applications such as field-effect transistors, photoelectric conversion devices, bio/chemical sensors and so forth [1–3]. To exploit nanostructured assemblies of these unique composites, the solubilization of carbon nanotubes is one of the important challenges because they have low solubility in most solvents. Many groups have explored the solubilization properties of carbon nanotubes upon chemical modification, which involves their covalent bonding to organic materials [4,5]. Recently, carbon nanotubes with covalently linked porphyrin antennae were introduced as potential supramolecular donor–acceptor complexes for applications such as photovoltaic devices and light-harvesting systems [6]. On the other hand, noncovalent functionalizations of surfactants or hydrophilic polymers such as poly(vinylpyrrolidone), poly (vinyl alcohol), or poly(ethylene oxide) on carbon nanotubes have also been studied as a simple method of obtaining suspensions in both water and organic solvents [7,8]. The solubilization of single-walled carbon nanotubes (SWNTs) with aromatic compounds such as porphyrin or polyfluorene has been reported [9–12]. The solubilization mechanism involved π–π interactions between the side walls of the SWNTs and the aromatic compounds, which play an important role in achieving supramolecular assemblies. Since charges can be injected from porphyrin into SWNTs upon the irradiation of light, the composites have been used as photochemical solar cells [13–15]. The use of a donor–acceptor system allows electron storage in SWNTs when in contact with photoirradiated TiO_2 nanoparticles [16]. We have also reported the micro/nanopatterning of SWNT–organic semiconductor composites using microcontact printing, dip-pen nanolithography and fountain-pen nanolithography [17].

A further important challenge for achieving optoelectronic device applications is the fabrication of nanostructured ultrathin films from SWNT–organic semiconductor composites. In this work, we report the fabrication of nanostructured SWNT–organic semiconductor ultrathin films by a layer-by-layer (LbL) self-assembly approach. The LbL self-assembly method, initially reported by Decher, is one of the most convenient techniques for fabricating molecularly controlled ultrathin multilayer films [18]. The adsorption process involves the alternate deposition of cationic and anionic species from a solution [19]. A number of groups have reported the LbL deposition of conducting organic and polymer materials [20–22]. However, there are also a few examples of LbL ultrathin films fabricated from SWNT–organic semiconductor molecules, particularly LbL ultrathin films fabricated via noncovalently solubilized SWNT–organic semiconductor composites. We used both positively and negatively charged water-soluble phthalocyanine

* Corresponding author.
E-mail address: ababa@eng.niigata-u.ac.jp (A. Baba).

0040-6090/$ – see front matter © 2009 Elsevier B.V. All rights reserved.
doi:10.1016/j.tsf.2009.09.052

molecules for the solubilization of SWNTs. To investigate the film fabrication, surface plasmon spectroscopy, UV–vis spectroscopy and cyclic voltammetric properties were studied.

2. Experimental details

2.1. Materials

SWNTs were purchased from Microphase Co. Copper phthalocyanine-3,4′,4″,4‴-tetrasulfonic acid tetrasodium salt (CuPS; Aldrich) and alcian blue, pyridine variant (AB; Aldrich) were obtained from Aldrich (shown in Fig. 1). For the functionalization of gold and glass slide substrates, 3-mercapto-1-propanesulfonic sodium and (3-aminopropyl) triethoxysilane (APS), obtained from Aldrich, were used, respectively.

2.2. Electrochemical measurements

All electrochemical measurements were carried out using a one compartment three-electrode cell driven by an HZ-5000 potentiostat (Hokuto Denko Ltd., Japan). In all measurements, the working electrodes consisted of gold films (d~50 nm) vacuum-evaporated onto a glass substrate (with an adhesion layer of 2 nm Cr previously evaporated onto the glass). The counter electrode was a platinum wire and the reference electrode was a Ag/Ag^+ non-aqueous electrode. All potentials reported in this paper are relative to this reference electrode. The gold electrode surface area was 0.785 cm^2.

2.3. Surface plasmon spectroscopy measurements

An attenuated total reflection setup was used for the excitation of surface plasmons in the Kretschmann configuration combined with a Teflon cell. A triangular S-LAH66 (OHARA) prism was used. The Au/glass substrates were clamped against the Teflon cell using an O-ring, which provided a liquid-tight seal. The Teflon cell was then mounted on a 2-axis goniometer for investigation by surface plasmon resonance spectroscopy (SPR). Surface plasmons were excited by reflecting p-polarized laser light from the Au-coated base of the prism. The excitation source employed was a He–Ne laser with $\lambda = 632.8$ nm. Kinetic measurements were performed to monitor the formation of the LbL film via reflectivity changes as a function of time. Angular measurements were also performed by monitoring the reflectivity as a function of incident angle θ_0. For these experiments, the gold film thickness (~47 nm) was chosen for optimum excitation of the surface plasmons. Details of the electrochemical-SPR setup can be found elsewhere [23,24].

2.4. Solubilization of SWNT–organic semiconductor composites

For the solubilization of SWNTs with organic semiconductors, 0.25 mg/ml SWNTs and 0.25 mg/ml AB or CuPS were mixed in deionized water, then they were sonicated for several hours. The obtained solution was centrifuged for 1 h to remove the aggregates or bundled complexes. The supernatant of the solution was used for the LbL deposition. The solubility of AB-SWNT and CuPS-SWNT composites was investigated by UV–vis absorption spectroscopy.

2.5. Layer-by-layer deposition

The LbL deposition of AB-SWNT and CuPS-SWNT was performed following the Decher approach [25]. The gold surface of the flat solid substrate was functionalized by the immersion of the slide for 1 h in an ethanol solution of 3-mercapto-1-propanesulfonic sodium salt (10 mg/ml) (followed by rinsing), thus creating a uniformly charged (negative) Au/Cr/glass substrate surface. The bare glass substrates were functionalized by APS (0.1% in toluene). The APS layer was charged by the immersion of the substrate in dilute HCl solution, which was used immediately for preparing the LbL ultrathin film. The Au/Cr/glass substrates or glass substrates with functionalized surfaces were alternately immersed for 20 min in aqueous solutions of AB-SWNT and CuPS-SWNT until the desired number of layers was achieved. Rinsing with deionized water for 2 min was carried out between depositions.

3. Results and discussion

3.1. Solubilization of SWNTs with water-soluble phthalocyanine

To examine the solubility of AB-SWNT and CuPS-SWNT composites, UV–vis absorption spectra were measured in an aqueous solution. Fig. 2(a) shows the UV–vis absorption properties of AB and AB-SWNT composites after sonication for 3 h and after sonication (3 h)/centrifugation (1 h at rotation speeds of 7000 and 10,000 rpm) in an aqueous solution. Fig. 2(b) shows the spectra for CuPS and CuPS-SWNT composites after sonication and after sonication/centrifugation. In the absorption spectra of both composites, peaks due to the Soret band (340–350 nm) and Q-band (610–620 nm) were clearly observed. After the sonication, an increase in the baseline of the broad absorption band was observed, indicating that both metallic SWNTs (400–600 nm region, corresponding to M_{11}) and semiconducting SWNTs (600–950 nm, corresponding to S_{22} transitions) were complexed with both AB and CuPS molecules. Since the bundles or aggregated complexes were mostly removed by centrifugation, the baseline gradually decreased as the rotation speed increased. On the other hand, the addition of SWNTs to AB or CuPS resulted in decreases in the peak intensity for both the Soret band and the Q-band, accompanied by a redshift of ca. 1 nm. These results suggest that an interaction between SWNTs and AB or CuPS is induced. The decrease in the peak intensities should be due to a decrease in the density of trapped electrons in AB or CuPS because they are transferred to SWNTs. Peak intensities then increased slightly as the rotation speed increased because of the removal of bundles or aggregates, in good agreement with the behavior of the baseline. Similar results were recently observed for SWNT–imidazole–porphyrin [13], SWNT–methyl viologen [14] and SWNT–TiO_2 [16] composites, which acted as donor–acceptor nanohybrid or electron storage systems in the SWNTs with Fermi level equilibration. Since a large number of SWNTs were removed at a higher rotation speed, a rotation speed of 6000 rpm was chosen for the fabrication of LbL films.

3.2. Fabrication of LbL ultrathin films

First, UV–vis spectroscopy was performed to monitor the AB-SWNT/CuPS-SWNT multilayer formation. As schematically shown in Fig. 1, 0.5 bilayer indicates 1 layer of AB-SWNT or CuPS-SWNT composites. As can be seen in Fig. 3, the change in absorbance for the first bilayer was larger than that for the subsequent bilayers. This result suggests that the AB-SWNT and CuPS-SWNT composites are poorly charged; thus, the amount of deposition on the APS-functionalized surface is larger than that on the composites. From second bilayer, the UV–vis absorbance exhibited a monotonic increase with the number of bilayers,as shown in the inset, suggesting the successive deposition of the film during the assembly of the multilayers. As discussed in the previous section, the UV–vis spectra of AB-SWNT and CuPS-SWNT in solution exhibited peaks at approximately 331 nm and 611 nm and at 338 nm and 630 nm, respectively. On the other hand, the Soret absorption band and Q-band in the multilayered film were observed at 334 nm and 619 nm, respectively, almost superpositions of the peaks due to the two phthalocyanine molecules (AB and CuPS). Furthermore, it should be noted that the baseline of the absorption at approximately 500 nm increased with the number of bilayers, while the baseline of the AB–CuPS LbL film (without

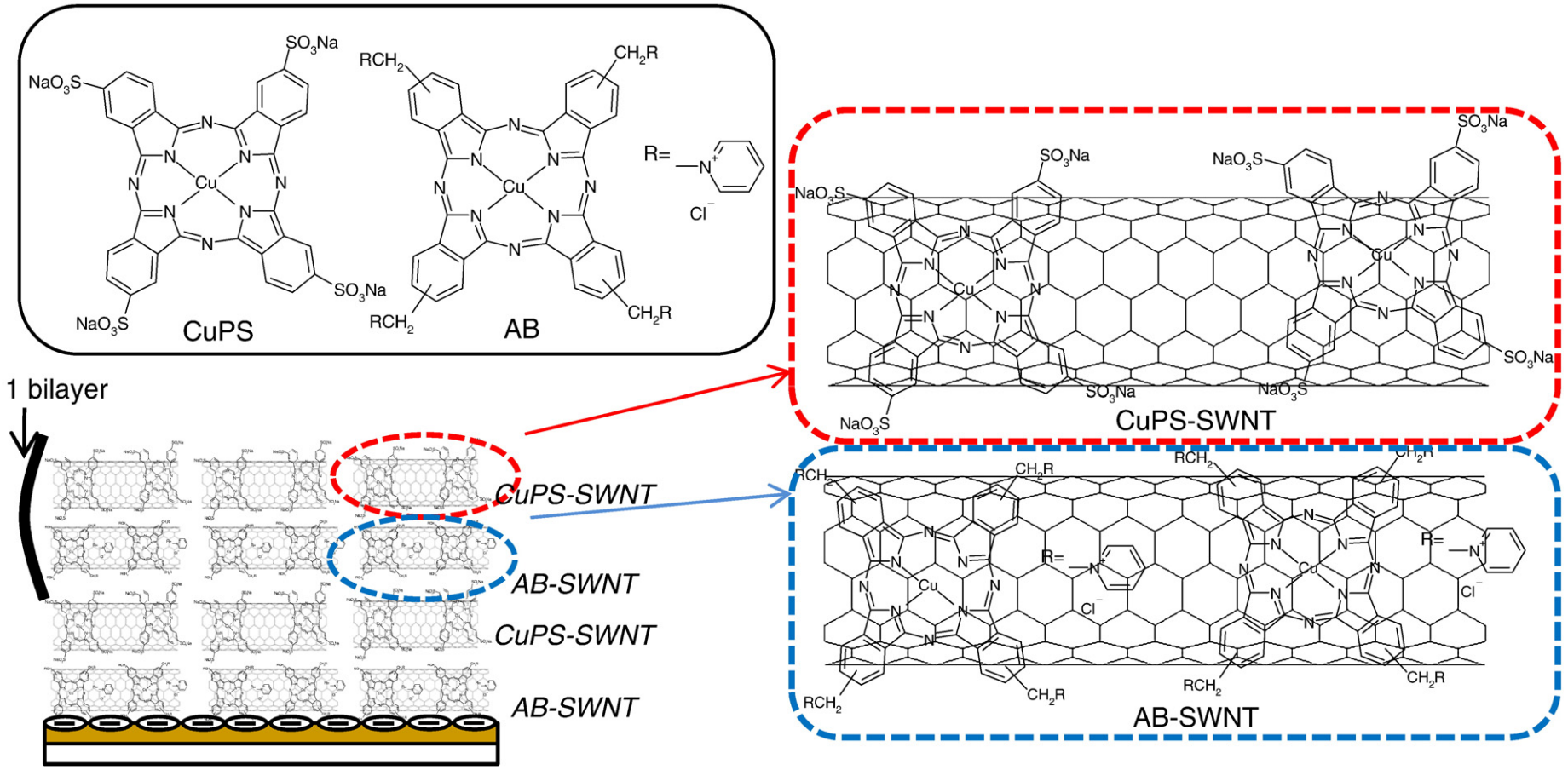

Fig. 1. Schematic drawing of the fabrication of nanostructured alcian blue, pyridine variant (AB)-SWNT/phthalocyanine-3,4′,4″,4‴-tetrasulfonic acid tetrasodium salt (CuPS)-SWNT LbL films.

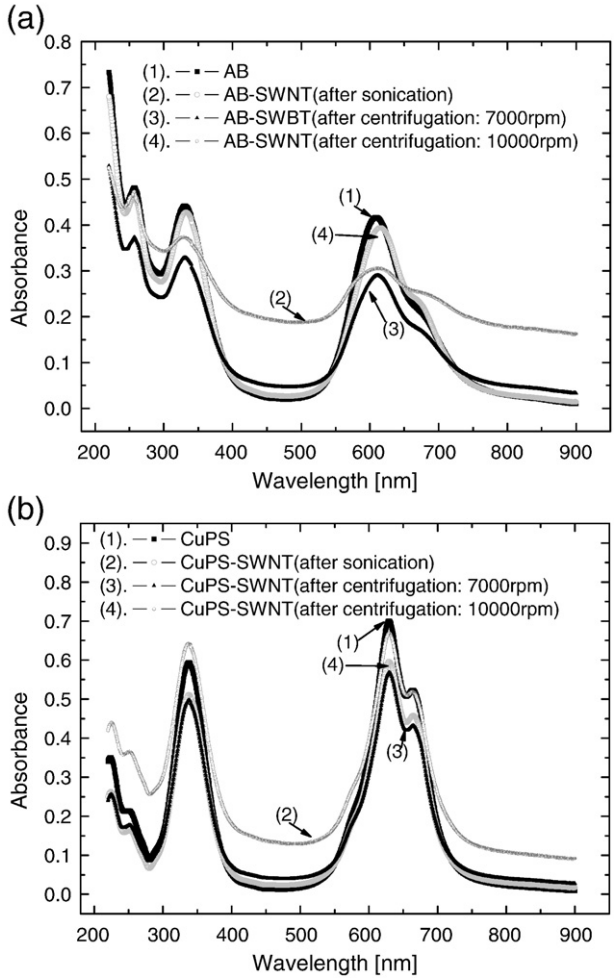

Fig. 2. UV–vis absorption properties. (a) AB (0.25 mg/ml) and AB (0.1 mg/ml)-SWNT (0.25 mg/ml) composites after sonication for 3 h and after sonication (3 h)/centrifugation (1 h at rotation speeds of 7000 and 10,000 rpm) in aqueous solution. (b) CuPS (0.25 mg/ml), CuPS (0.25 mg/ml)-SWNT (0.25 mg/ml) composites after sonication for 3 h, and after sonication (3 h)/centrifugation (1 h at rotation speeds of 7000 and 10,000 rpm) in aqueous solution.

SWNTs) remained almost constant (see supporting information), indicating that a well-ordered SWNT–phthalocyanine composite film was fabricated.

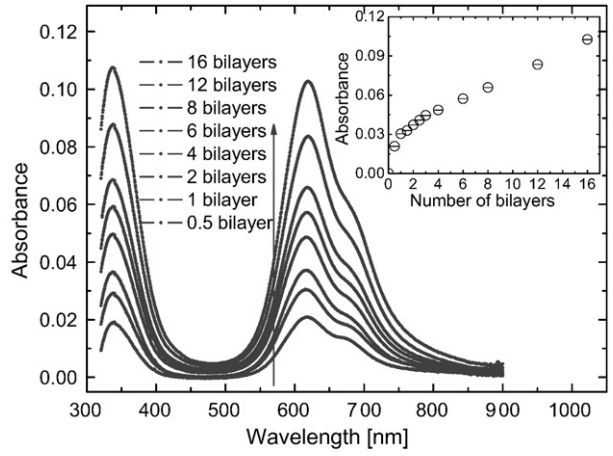

Fig. 3. UV–vis spectrum of AB-SWNT/CuPS-SWNT LbL film on glass slide as a function of number of bilayers. (0.5 bilayer indicates 1 layer of AB-SWNT (or 1 layer of CuPS-SWNT).) The inset shows the absorbance of the UV–vis peaks at 617.5 nm as a function of a number of bilayers.

SPR spectroscopy was also employed in order to study the *in situ* adsorption process of the composites. Fig. 4(a) shows the change in reflectivity measured *in situ* by SPR at a fixed incident angle of 61° during the multilayer fabrication process. As can be seen in this figure, the reflectivity change in the first bilayer indicated large amount of adsorption onto the surface, which corresponded to the result of UV–vis spectroscopy. The stepwise increase in reflectivity with increasing number of bilayers indicates the deposition of a constant amount of AB-SWNT/CuPS-SWNT. For each bilayer, the change in reflectivity change due to AB-SWNT is larger than that due to CuPS-SWNT, indicating that a larger amount of AB-SWNT is deposited. This might be due to the charge balance between AB and CuPS molecules. The decrease in reflectivity during the deposition of each layer indicates that some desorption of the composites occurs during this process. The kinetic data also show that the thickness of each layer can be controlled by changing the immersion and rinsing times of each composite [19], [26]. Since each monolayer of the layer-by-layer film consists of SWNT–phthalocyanine composites, the packing density might be markedly affected by the immersion time. As shown in Fig. 4(b), the angular SPR reflectivity curve exhibits a shift of about 3° toward a higher angle after the deposition of 5 bilayers. The film thickness of the 5-bilayer film was estimated to be ca. 14.0 nm on the assumption of a dielectric constant of 2.1 + i0.2, giving an average thickness of 2.8 nm for each bilayer. Since the depth of the SPR curve mainly depends on the absorption of the deposited film, the shallow and broadened curve is due to the Q-band absorption (i.e., close to the probing wavelength of 633 nm) of the deposited film.

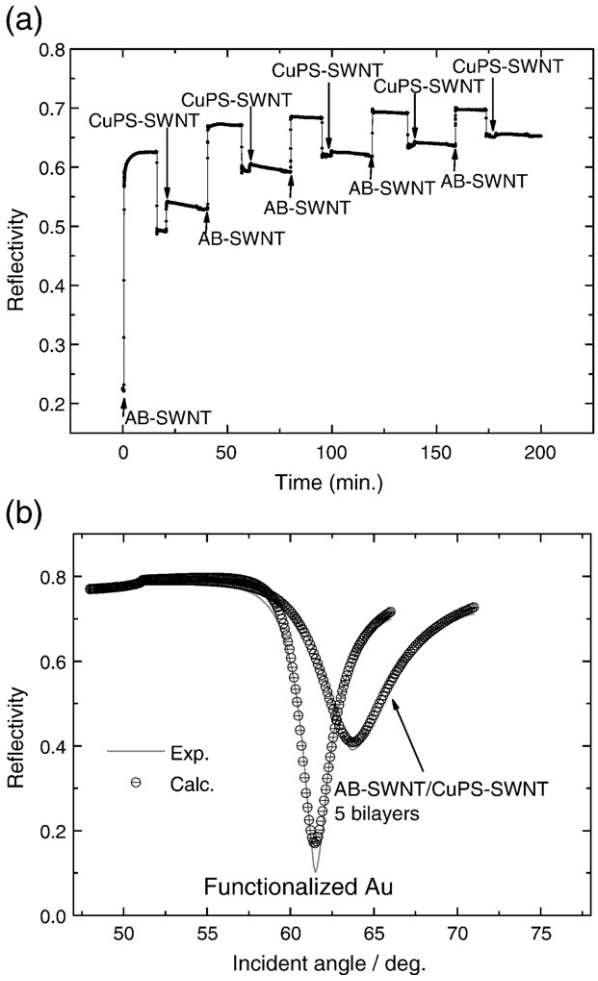

Fig. 4. (a) *In situ* surface plasmon resonance kinetic reflectivity curve during the deposition of AB-SWNT/CuPS-SWNT LbL film. (b) Angular SPR reflectivity curves measured before and after the deposition of 5 bilayers of AB-SWNT/CuPS-SWNT LbL film.

3.3. Cyclic voltammetry of LbL ultrathin films

To study the effect of the SWNTs in the composite LbL system, three different structures were fabricated, i.e., 10-bilayer AB/CuPS films (no SWNTs), films with 5 AB-SWNT/CuPS-SWNT bilayers and 5 AB/CuPS bilayers (50% composite), and 10-bilayer AB-SWNT/CuPS-SWNT composite films (100% composite) as schematically shown in the inset of Fig. 5. Cyclic voltammetry for the three structures was performed in acetonitrile with a supporting electrolyte of 0.1 M tetrabutylammonium hexafluorophosphate ($TBAPF_6$) as a function of scan rate up to 300 mV/s in the potential range of 0 to 1.0 V. As shown in the figure, an oxidation peak was clearly observed at approximately 0.6 V for the LbL films with SWNTs, while the AB/CuPS film exhibited a low oxidation/reduction current. Since the SWNTs do not exhibit a redox peak in this range, this result indicates that SWNTs can enhance the electroactivity of phthalocyanine multilayer films fabricated by the proposed simple technique. The peak current gradually shifted toward a higher potential with increasing scan rate, indicating the kinetic limitation of the system [27]. Furthermore, the peak current of the SWNT composite film was larger than that of the film without SWNTs. As the film thickness was estimated to be about the same for each structure, the enhanced electroactivity should be attributed to the effect of the SWNTs in the film. From these peak currents, the scan rate dependence was plotted for each structure (Fig. 6). As shown in this figure, all the plots are linear in the scan rate, which indicates a surface-controlled process for all structures [28]. Furthermore, the slopes obtained from the peak currents indicate that the SWNT–phthalocyanine composite film has a high electron transfer rate [29].

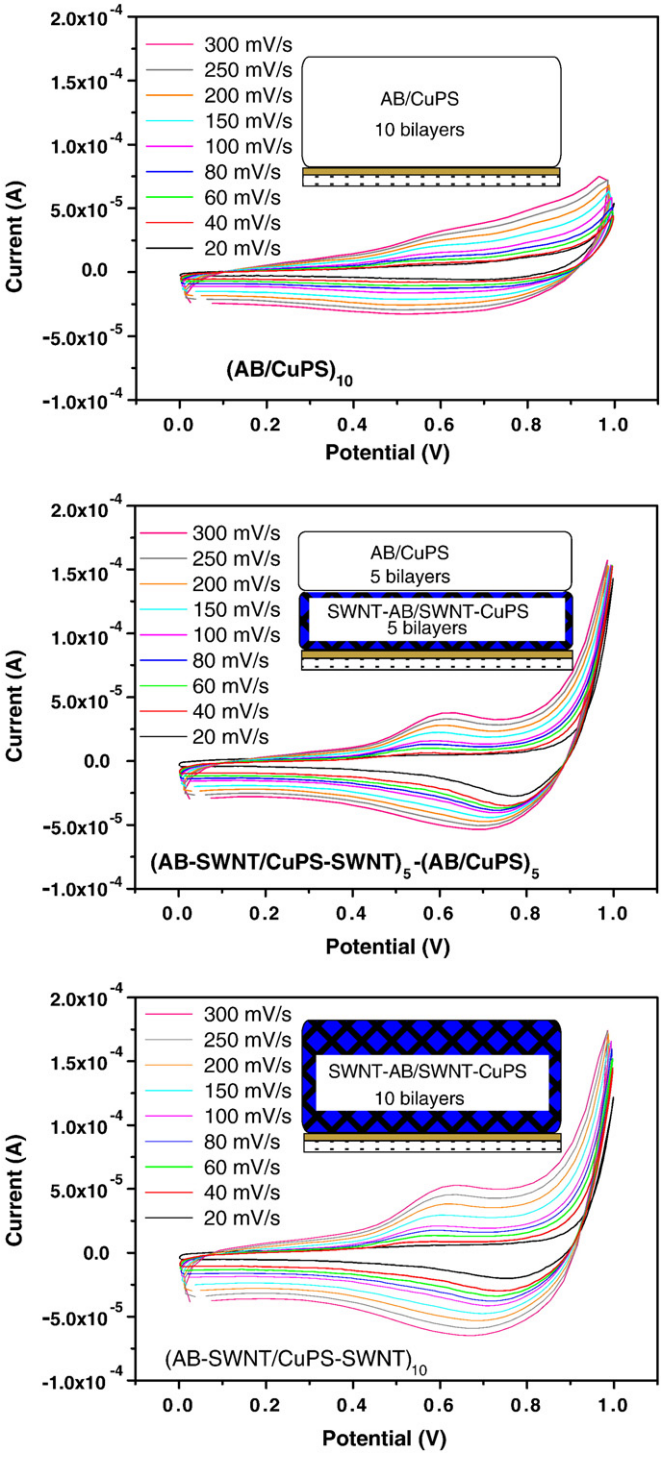

Fig. 5. Cyclic voltammetry properties of three different film structures, i.e. 10-bilayer AB/CuPS films, films with 5 AB-SWNT/CuPS-SWNT bilayers and 5 AB/CuPS bilayers, and 10-bilayer AB-SWNT/CuPS-SWNT composites, in acetonitrile containing 0.1 M $TBAPF_6$ at scan rates from 20 to 300 mV/s.

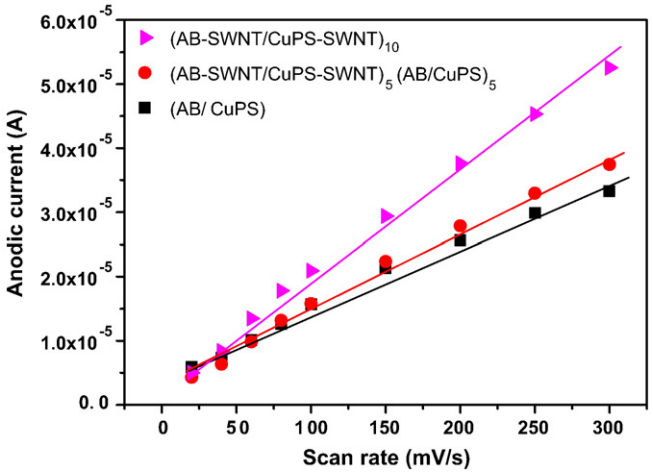

Fig. 6. Relationship between anodic peak current and scan rate.

4. Conclusions

We have demonstrated a convenient method for fabricating nanostructured carbon nanotube-organic semiconductor hybrid ultrathin films via the noncovalent adsorption of composites. SWNTs were solubilized with water-soluble charged phthalocyanine molecules, which were then used for electrostatic LbL multilayer fabrication. The results of UV–vis spectroscopy revealed the deposition of composite films. *In situ* SPR spectroscopy during the layer-by-layer multilayer fabrication indicated a stepwise increase in reflectivity, indicating the successive formation of nanostructured hybrid ultrathin films. Cyclic voltammetry revealed that the electroactivity of the hybrid film was enhanced by the SWNTs. The slopes obtained from the peak currents for three film structures exhibited that the SWNTs facilitated the electron transfer to the electrode, which should have the potential for device applications.

Acknowledgements

This work was partly supported by a Grant-in-Aid for Scientific Research from the Japan Society for the Promotion of Science and a Grant for the Promotion of Niigata University Research Projects.

References

[1] S. Liu, S.C.B. Mannsfeld, M.C. LeMieux, H.W. Lee, Z. Bao, Appl. Phys. Lett. 92 (2008) 053306.
[2] C. Klinke, J.B. Hannon, A. Afzali, P. Avouris, Nano Lett. 6 (2006) 906.
[3] R.J. Chen, S. Bangsaruntip, K.A. Drouvalakis, N.W.S. Kam, M. Shim, Y.M. Li, W. Kim, P.J. Utz, H.J. Dai, Proc. Natl Acad. Sci. USA 100 (2003) 4984.
[4] J. Chen, M.A. Hamon, H. Hu, Y. Chen, A.M. Rao, P.C. Eklund, R.C. Haddon, Science 282 (1998) 95.
[5] D. Baskaran, J.W. Mays, X.P. Zhang, M.S. Bratcher, J. Am. Chem. Soc. 127 (2005) 6916.
[6] D.M. Guldi, G.M.A. Rahman, V. Sgobba, C. Ehl, Chem. Soc. Rev. 35 (2006) 471.
[7] V.C. Moore, M.S. Strano, E.H. Haroz, R.H. Hauge, R.E. Smalley, Nano Lett. 3 (2003) 1379.
[8] V.A. Sinani, M.K. Gheith, A.A. Yaroslavov, A.A. Rakhnyanskaya, K. Sun, A.A. Mamedov, J.P. Wicksted, N.A. Kotov, J. Am. Chem. Soc. 127 (2005) 3463.
[9] H. Murakami, T. Nomura, N. Nakashima, Chem. Phys. Lett. 378 (2003) 481.
[10] Y. Tomonari, H. Murakami, N. Nakashima, Chem. Eur. J. 12 (2006) 4027.
[11] N. Nakashima, Sci. Tech. Adv. Mater. 7 (2006) 609.
[12] A. Nish, J.Y. Hwang, J. Doig, R.J. Nicholas, Nat. Mater. 2 (2007) 640.
[13] R. Chitta, A.S.D. Sandanayaka, A.L. Schumacher, L.D. D'Souza, Y. Araki, O. Ito, F. D'Souza, J. Phys. Chem. C 111 (2007) 6947.
[14] D.M. Guldi, G.M.A. Rahman, N. Jux, D. Balbinot, N. Tagmatarchis, M. Prato, Chem. Commun. 15 (2005) 2038.
[15] T. Hasobe, S. Fukuzumi, P.V. Kamat, J. Phys. Chem. B 110 (2006) 25477.
[16] A. Kongkanand, P.V. Kamat, ACS Nano 1 (2007) 13.
[17] A. Baba, F. Sato, N. Fukuda, H. Ushijima, K. Yase, Nanotechnology 20 (2009) 085301.
[18] G. Decher, Science 277 (1997) 1232.
[19] A. Baba, F. Kaneko, R.C. Advincula, Colloids Surf. A 173 (2000) 39.
[20] A. Baba, M.K. Park, R.C. Advincula, W. Knoll, Langmuir 18 (2002) 4648.
[21] J.H. Cheung, A.F. Fou, M.F. Rubner, Thin Solid Films 244 (1994) 985.
[22] L. Zhai, R.D. McCullough, Adv. Mater. 14 (2002) 901.
[23] A. Baba, J. Lübben, K. Tamada, W. Knoll, Langmuir 19 (2003) 9058.
[24] A. Baba, Y. Sano, Y. Ohdaira, K. Shinbo, K. Kato, F. Kaneko, IEICE Trans. Electron. E91-C (2008) 1881.
[25] G. Decher, J.D. Hong, Makromol. Chem. Makromol. Symp. 46 (1991) 321.
[26] Y. Okayama, T. Ito, S. Shiratori, Thin Solid Films 393 (2001) 132.
[27] V.S. Vasantha, S.M. Chen, Electrochim. Acta 51 (2005) 347.
[28] R. Baker, D.P. Wilkinson, J. Zhang, Electrochim. Acta 53 (2008) 6906.
[29] U. Yogeswaran, S.M. Chen, Electrochim. Acta 52 (2007) 5985.